Rhizobial effector NopM ubiquitinates Nod factor receptor NFR5 and promotes rhizobial infection in *Lotus japonicus*

Yanan Wang[1], Hanbin Bao[1], Yutao Lei[1], Lifa Yuan[1], Haoxing Li[1], Hui Zhu[1], Dawei Xin[2], Christian Staehelin[3], and Yangrong Cao[1]*

[1] National Key Lab of Agricultural Microbiology, Hubei Hongshan Laboratory, Huazhong Agricultural University, Wuhan, Hubei, 430070, China.

[2] Key Laboratory of Soybean Biology of Chinese Ministry of Education, Key Laboratory of Soybean Biology and Breeding/Genetics of Chinese Agriculture Ministry, Northeast Agricultural University, Harbin, Heilongjiang, 150038, China.

[3] State Key Laboratory of Biocontrol and Guangdong Key Laboratory of Plant Resources, School of Life Sciences, Sun Yat-sen University, Guangzhou, 510275, China.

*Corresponding author: Yangrong Cao

Email: yrcao@mail.hzau.edu.cn

Abstract

Bacterial pathogens and nitrogen-fixing rhizobia employ type III protein secretion system (T3SS) effectors as potent tools to manipulate plant signaling pathways, thereby facilitating infection and host colonization. However, the molecular mechanisms underlying effects of rhizobial effectors on legume infection remain largely elusive. In this study, we investigated the symbiotic role of T3SS effectors in the interaction between *Sinorhizobium fredii* NGR234 and *Lotus japonicus*. Mutants deficient in the T3SS genes *Tts1* or *NopA* showed enhanced rhizobial infection of *L. japonicus* roots. Further mutant analysis showed that the NopT effector negatively affects infection, while the NopM effector in the absence of NopT promotes infection. Notably, NopM interacts

with the Nod factor receptors LjNFR1 and LjNFR5. NopM ubiquitinates LjNFR5 with ten ubiquitinated lysine residues in LjNFR5 identified using mass spectrometry. Expression of *NopM* in *L. japonicus* resulted in an approximately twofold increase in LjNFR5 protein levels and enhanced rhizobial infection. Our findings indicate that NopM directly interferes with the symbiotic signaling pathway through interaction and ubiquitination of Nod factor receptors, which likely benefits rhizobial infection of *L. japonicus*. Our research contributes to the intricate interplay between the Nod factor signaling pathway and rhizobial T3SS effectors delivered into host cells.

Keywords: Legume–rhizobium symbiosis; rhizobial effector; NopM; Nod factor receptors.

Introduction

The legume-rhizobium symbiosis leads to the formation of nodules, where rhizobia reside and reduce nitrogen into ammonia, nutrilizing the plants. Nodule formation depends on complicated regulations and mutual signal exchanges between hosts and symbionts. Legume roots release flavonoids, which might activate NodD transcriptional regulators, initiating the expression of genes for type III protein secretion system (T3SS) and biosynthesis of lipo-chitooligosaccharides known as Nod factors (NFs) (Yang et al., 2022). These NFs are recognized by Nod factor receptors (NFRs) in host plants, such as LjNFR1 and LjNFR5 in *Lotus japonicus*, activating symbiotic signaling pathways crucial for successful nodulation (Radutoiu et al., 2003).

Similar to gram-negative bacterial pathogens whose type III protein secretion system (T3SS) effectors are vital for interacting with host pathways, rhizobia inject effector proteins into plant cells to promote rhizobial symbiosis and/or suppress plant immunity (Teulet et al., 2022). The expression of rhizobial genes

related to T3SS and effectors is induced by flavonoid-NodD complex and TtsI (Wassem et al., 2008). These T3SS components and effectors, termed nodulation outer proteins (Nops), have been implicated in infection, nodulation, and host specificity (Deakin & Broughton, 2009; Teulet et al., 2022). The symbiosis promoting effects of translocated effectors are often attributed to the suppression of host defense reactions, while negative (asymbiotic) effects may be the result of direct or indirect recognition of effectors by intracellular resistance proteins (Teulet et al., 2022).

Several Nops have been characterized biochemically to date. For instance, *Sinorhizobium fredii* NGR234, a strain with broad-host range, has been well-studied. NopA (Deakin et al., 2005) and NopB (Saad et al., 2005) are major components of the T3SS complex and interact physically with NopX, facilitating the translocation of effector proteins into plant cells (Büttner et al., 2002). NopL, known to delay nodule senescence in bean, acts as a mitogen-activated protein kinase (MAPK) substrate and reduces levels of pathogenesis-related (PR) proteins in plants (Ge et al., 2016, Bartsev et al., 2004). NopP synergistically promotes nodulation with NopL and is phosphorylated by unknown kinases (Skorpil et al., 2005). NopT, a cysteine protease, regulates symbiosis between NGR234 and various hosts (Dai et al., 2008), triggering rapid cell death dependent on its protease activity (Dai et al., 2008). Additionally, NopT cleaves both LjNFR5 and GmPBS1, regulating plant symbiotic signaling and defense responses, respectively (Khan et al., 2022, Li et al., 2023). NopM, an E3 ubiquitin ligase, dampens flagellin-induced immunity and interferes with MAPK signaling (Xu et al., 2018).

While effectors of bacterial pathogens in plant pathogenesis are known to target plant components of pattern-triggered immunity pathway to favor pathogenic infection, it remains unknown whether rhizobial effectors function similarly regulating symbiotic signaling pathway. Here, we investigated the function of

91 T3SS effectors from *S. fredii* NGR234 in the interaction with *L. japonicus* and
92 found that the T3SS negatively affects rhizobial infection in this plant. Further
93 mutant analysis showed that NopT suppresses rhizobial infection, whereas
94 NopM (in the absence of NopT) promoted infection. NopM interacts with
95 LjNFR1 and LjNFR5. But NopM selectively ubiquitinates LjNFR5, increasing
96 LjNFR5 protein levels. Transgenic plants expressing NopM showed increased
97 infection events and a higher number of nodule primordia. These findings
98 establish a direct link between rhizobial effectors and the symbiotic signaling
99 pathway, providing crucial insights into the mechanisms of legume-rhizobium
100 symbiosis.
101
102 **Materials and Methods**
103
104 Plant Materials and Inoculation with Rhizobia
105
106 *Lotus japonicus* Gifu B–129 ecotype was provided by the Center for
107 Carbohydrate Recognition and Signaling (https://lotus.au.dk/), and used for
108 phenotype analysis. *L. japonicus* Gifu *nfr 5* mutant (Radutoiu et al., 2003) and
109 Gifu *proNIN:GUS* transgenic line (Heckmann et al., 2011). Wild type plants of
110 *L. japonicus* 'Miyakojima' MG20 were used for phenotype analysis and stable
111 transformation. Transgenic *L. japonicus* MG20 plants overexpressing *LjNFR5*
112 from a *Ubiquitin* promoter (encoding HA-tagged LjNFR5) were constructed in
113 our laboratory and used for hairy root transformation (*proUbiquitin:LjNFR5-HA*
114 line).
115
116 All *L. japonicus* seeds were surface-sterilized with H_2SO_4 for 6 min, and then
117 with 2 % (w/v) NaClO for 6 min. After synchronization of germination at 4 °C in
118 the dark for 2 days, the seeds were placed on Murashige & Skoog (MS) medium
119 (PhytoTech, M519) containing 1.5 % (w/v) agar for germination (22°C for 2 days
120 in the dark and 2 days in the light). Seedlings were then transferred to growth

121 pots containing vermiculite supplied with ½ B&D (Broughton & Dilworth)
122 medium (Broughton and Dilworth, 1971) without nitrogen. Plants were kept
123 under long–day conditions (16 h light/ 8 h dark) at 22 °C. For infection
124 experiments, seven-day-old seedlings were inoculated with *S. fredii* NGR234
125 and NGR234 mutants or *M. loti* MAFF303099 (OD_{600}=0.02).
126
127 Plasmid Construction
128
129 All plasmids used in this study were generated using MultiF Seamless
130 Assembly Mix (ABclonal, China, RK21020). Plasmids pG5XX–HA, pG5XX–
131 Myc, pG5XX–FLAG, pG5XX–nLUC, pG5XX–cLUC, pG5XX–GFP (Bao et al.,
132 2024), point mutant *LjNFR1*^{K351E} and point mutant *NopM*^{C338A} using overlapping
133 PCR were generated. To detect the interaction between *LjNFR1*, *LjNFR5*, and
134 *NopM*^{C338A} in *Nicotiana benthamiana* in split-luciferase complementation
135 experiments, the full–length coding sequences of *LjNFR1*, *LjNFR1*^{K351E},
136 *LjNFR5*, *NopM*^{C338A}, and *AtFLS2* were cloned into *Xba*I-*Kpn*I digested pG5XX–
137 nLUC (Wang et al., 2021) and pG5XX–cLUC (Wang et al., 2021), respectively.
138 For BIFC experiments, the full–length coding sequences of *LjNFR1*, *LjNFR5*,
139 *NopM*^{C338A}, and *AtFLS2* were cloned into pSPYCE (MR) (Waadt et al., 2008)
140 and pSPYNE (R)173 (Waadt et al., 2008), respectively, between *Xba*I and
141 *Bam*HI. For the co-IP assay, the full–length *LjNFR1*, *LjNFR5*, *NopM*^{C338A} coding
142 sequences were cloned into pG5XX–GFP, pG5XX–FLAG, respectively,
143 between *Xba*I and *Kpn*I. For the pull-down assay with *E. coli,* the sequence
144 encoding the cytosolic domain of *LjNFR5* fused to a Myc tag was cloned into
145 plasmid pMAL-c2X (Addgene, 75286) between *Bam*HI and *Hind*III and the
146 *NopM* coding sequence was cloned into plasmid pACYCDuet ((Han et al., 2017)
147 between *Sgs*I and *Not*I. The *Myc* tag was cloned from pG5XX–Myc and inserted
148 into plasmid pMAL-c2X between *Bam*HI and *Hind*III, generating plasmid pMAL-
149 c2X-Myc used as control. For *in vitro* ubiquitin assay in *E. coli*, *NopM* or
150 *NopM*^{C338A}, and Myc tagged cytosolic domain (CD) of NFR5 (NFR5^{CD}-Myc/

151 LjNFR5^{10KR}-Myc) were inserted into plasmid pACYDuet and pCDFDuet ((Han
152 et al., 2017) between *Sgs*I and *Not*I respectively. His and FLAG tagged ubiquitin
153 (His-FLAG-Ub^{K0}) was generated by GenScript Biotech. For hairy roots
154 transformation of *L. japonicus*, the plasmid pUB-RFP (Feng et al., 2021) was
155 digested with *Kpn*I and *Xba*I, and was inserted fragment *NopM* and *NopM^{C338A}*.
156 For stable transformation in *L. japonicus NopM* was cloned into *Kpn*I-*Xba*I
157 digested pUB-Hyg-FLAG (Feng et al., 2021), generating plasmid pUB-Hyg-
158 NopM-FLAG with a *Ubiquitin* promoter. A 3-kb promoter fragment upstream of
159 the start codon of *NIN* was then cloned from genomic *L. japonicus* MG20 DNA
160 and inserted into *Xba*I- *Pst*I digested pUB-Hyg-NopM-FLAG to replace the
161 *Ubiquitin* promoter. The resulting plasmid was named proNIN-NopM-Hyg-FLAG.
162 All primers used are listed in the Supplementary Table S1.
163
164 Stable Transformation in *L. japonicus*
165
166 The plasmid proNIN-NopM-Hyg-FLAG was transformed into *L. japonicus* MG20
167 seedlings using *Agrobacterium tumefaciens* strain EHA105 as described by
168 Handberg and Stougaard (Handberg & Stougaard, 1992). 50 mg/ml
169 hygromycin B (Sangon Biotech, China, A600230) was used for selection of
170 transgenic plants. The final positive transgenic plants were detected by PCR
171 analysis.
172
173 Transient Expressing in *N. benthamiana* Leaves
174
175 *A. tumefaciens* EHA105 strains carrying various constructs were cultivated
176 overnight and resuspended with an *Agrobacterium* culture harboring the P19
177 suppressor with the ratio 1:1 in infiltration buffer (10 mM $MgCl_2$, 10 mM MES
178 pH=5.8 and 100 μM acetosyringone). The bacterial suspensions were infiltrated
179 into leaves of 4–week–old *N. benthamiana* plants. Leaves were harvested for
180 two days post infiltration.

181

182 BiFC and Split Luciferase Assays

183

184 In the BiFC assay with transformed *N. benthamiana* leaves, the eYFP
185 fluorescence of fusion proteins was analyzed 2–3 days after infiltration using a
186 confocal microscope (Leica TCS SP8).

187

188 In the split–luciferase assay, the plasmids were transformed into *N.*
189 *benthamiana* leaves using *Agrobacterium* strain EHA105. Three days after
190 infection, leaves were sprayed with 1 mM luciferin (Promega, E1603) and 0.02 %
191 (v/v) Triton X–100. The LUC activity was detected using the Tanon Imaging
192 system (Tanon, China, 4600).

193

194 Co-IP and Pull-down Assays

195

196 For the co-IP assay, total proteins were extracted from the *N. benthamiana*
197 leaves in IP buffer (50 mM Tris-HCl, pH=7.4, 150 mM NaCl, 1 mM EDTA, 1 %
198 TritonX-100, 5 % glycerol) supplemented with a protease inhibitor cocktail
199 (Yuanye, China, S25910). Samples were incubated at 4 °C for 10 min and
200 centrifuged at 12,000 × g for 10 min at 4 °C. The supernatant was added to
201 10 μL anti-GFP Nanobody Agarose Beads (Alpa Life Bio, KTSM1301) and
202 incubated at 4 °C for 3 h. The beads were washed at least five times with
203 washing buffer (50 mM Tris-HCl, pH=7.4, 150 mM NaCl, 1 mM EDTA). Western
204 blotting was detected by anti-GFP (ABclonal, China, AB_2770402) and anti-
205 FLAG (Sigma, F1804) antibodies.

206

207 For the pull-down assay with *E. coli* BL21 (DE3), protein synthesis of co-
208 expressed MBP-LjNFR5^{CD}-Myc or MBP-Myc and His-NopM was induced with
209 0.5 mM IPTG and incubation at 28 °C for 18 h. MBP-LjNFR1^{CD}-Myc, or MBP-
210 Myc and His-NopM were co–expressed in a similar way but bacteria were kept

211 at 18 °C for 20 h. Total proteins were extracted from *E. coli* in column buffer (20
212 mM Tris-HCl, pH=7.4, 0.2 M NaCl, 1 mM EDTA). Samples were centrifuged at
213 12,000 × g for 10 min at 4 °C. The supernatant was added to 20 μL amylose
214 resin beads (New England Biolabs, E8022S) and incubated at 4 °C for 3 h. The
215 beads then were washed at least five times with column buffer. Western blotting
216 was detected by anti-Myc (Bio Legend, 626808) antibody and anti-NopM
217 antibody kindly provided by Dr. Xin from North East Agriculture University.
218
219 *In Vitro* Ubiquitination Assay
220
221 The *in vitro* ubiquitination assay was performed using genes encoding AtUBA1
222 (E1), AtUBC8 (E2), NopM (or $NopM^{C338A}$), ubiquitin (or His-FLAG-Ub^{K0}) and the
223 cytosolic domain of LjNFR5 (or LjNFR1) as described previously (Han et al.,
224 2017). Different combinations of vectors were transformed into the *E. coli* BL21
225 (DE3). Recombinant protein expression was induced with 0.5 mM IPTG and
226 cells were grown at 28 °C for 20 h. The cell lysates were subjected to Western
227 blotting analysis using anti-Myc (Bio Legend, 626808) antibody, anti-FLAG
228 (Sigma, F1804) antibody, and anti-NopM antibody.
229
230 Generation of Hairy Roots Expressing NopM and $NopM^{C338A}$ in *L. japonicus*
231
232 The pUB-RFP vectors carrying *NopM* and $NopM^{C338A}$ were transformed into
233 *proUbiquitin:LjNFR5-HA* seedlings and Gifu seedlings using *A. rhizogenes*
234 LBA1334 (Feng et al., 2021). The *proLjNFR5:LjNFR5-GFP* and
235 *proLjNFR5:LjNFR5*^{10KR}*-GFP* vectors were transformed into Gifu *nfr5* seedlings
236 using *A. rhizogenes* LBA1334. The expression of RFP and GFP markers
237 enabled selection of transgenic hairy roots using a fluorescence stereo
238 microscope (Nikon, SMZ18).
239
240 Analysis of proteins expressed in *L. japonicus*

241

242 Total proteins were extracted from transgenic hairy roots using IP buffer (20 mM
243 Tris–HCl pH=7.5, 50 mM NaCl, 1 mM EDTA, 0.1 % SDS, 1 % Triton X-100)
244 supplemented with a protease inhibitor cocktail (Yuanye, China, S25910).
245 Western blotting was performed with anti-HA–peroxidase (Sigma, clone 3F10),
246 anti-actin (ABclonal, China, AC009), and anti-NopM antibodies.

247

248 NGR234 mutants Construction

249

250 *S. fredii* NGR234 derivatives with mutated *NopL (*NGRΩ*nopL*) (Marie et al.,
251 2003), and *NopT* (NGRΔ*nopT*) (Dai et al., 2008) have been constructed
252 previously. Additional mutations in the symbiotic plasmid of NGR234 were
253 generated by homologous recombination using the suicide vector pJQ200SK
254 (Quandt & Hynes, 1993). *S. fredii* NGR234 derivatives with mutated *NopJ*
255 *(*NGRΩ*nopJ*) was provided by Christian Staehelin.

256

257 NGR234 derivatives with mutated *TtsI*, *NopA*, *NopM*, *NopP* or *NopZ* (y4yJ)
258 genes, as well as double mutants with mutated *NopJ*, *NopL*, *NopM, NopP* or
259 *NopZ* genes in the *ΔnopT* background, were generated as follows (Fig. S1).
260 Firstly, a homologous recombination plasmid was constructed. A kanamycin
261 fragment cloned from plasmid pENTR/D-TOPO (Invitrogen, K240020SP) was
262 inserted into pJQ200SK digested with *Pst*I and *Bam*HI, yielding plasmid
263 pJQ200SK-Kan. A *Paph* promoter fragment cloned from plasmid pRJPaph-
264 bjGFP (Addgene, 67032) was then inserted into pJQ200SK-Kan digested with
265 *Pst*I, yielding plasmid pJQ200SK-*proKan:Kan* with a kanamycin resistance
266 interposon (ΩKan). A PCR-amplified 500-bp genomic NGR234 sequence
267 upstream of nucleotide position 18-21 of a given coding sequence and a
268 corresponding 800-bp genomic NGR234 sequence downstream of this position
269 were chosen as homologous arms. Plasmid pJQ200SK-*proKan:Kan* was
270 digested with *Pst*I, *Xho*I, *Bam*HI, and *Xba*I. The 500-bp upstream sequence

271 was cloned into the *Pst*I-*Xho*I site, and the 800-bp downstream sequence was
272 cloned into the *Bam*HI-*Xba*I site, generating a pJQ200SK-Ω plasmid with
273 homologous arms. Finally, the constructed plasmids were mobilized from *E. coli*
274 DH5a into NGR234 or the *ΔnopT* mutant by triparental mating using the
275 pRK2013 helper plasmid (Figurski and Helinski, 1979). Gene replacement was
276 forced by selecting for the resistance of the Ω interposon marker and for growth
277 on 5 % (w/v) sucrose. Double-crossover events at homologous sites were
278 confirmed by PCR analysis using genomic DNA extracted by a sodium dodecyl
279 sulfate (SDS) method (Fig. S2). Primers used are listed in Supplementary Table
280 S1 and constructed mutants in Supplementary Table S2.
281
282 To observe infection events, GFP-labeled strains were constructed. A GFP-
283 containing derivative of plasmid pHC60 (NovoPro, V005592) was mobilized into
284 NGR234 and the mutants by bacterial conjugation (Gross & Caro, 1966). GFP-
285 labeled colonies were detected by a fluorescence microscope (Nikon SMZ18).
286
287 GUS Staining
288
289 Roots were stained overnight in X-Gluc solution (50 mM sodium phosphate
290 pH=7.0, 50 mM EDTA pH=8.0, 0.5 mM $K_3Fe(CN)_6$, 0.5 mM $K_4Fe(CN)_6$, 0.1%
291 Triton X-100, 1 mM X-Gluc, 20 % methanol) at 37 °C. The chlorophyll was
292 removed by incubating the samples in 70 % ethanol. Images of roots were
293 taken using a fluorescence stereo microscope (Nikon, SMZ18).
294
295 Gene Expression Analysis
296
297 Total RNA was isolated using Plant RNA Kit (Yeasen, China, 19291ES50) from
298 transgenic hairy roots in plate selected by 50 mg/ml hygromycin B (Sangon
299 Biotech, China, A600230) inoculated *M. loti* MAFF303099 (OD_{600}=0.02) for 48
300 h. The total RNA (1 μg) was used for gDNA removal and cDNA synthesis using

301 the ABScript III RT Master Mix for qPCR with gDNA Remover (ABclonal, China,
302 RK20429). The cDNA was used as template for RT-PCR using 2X Universal
303 SYBR Green Fast qPCR Mix (ABclonal, China, RK21203). ATPase was used
304 as the reference gene. The primer sequences used for RT-PCR were listed in
305 Supplementary Table S1.
306
307 Sequence Alignment and Phylogenetic Analysis of NopM Orthologs
308
309 The protein sequences of NopM orthologs were retrieved using the BLASTP
310 program at the National Center for Biotechnology Information (NCBI)
311 (https://blast.ncbi.nlm.nih.gov/Blast.cgi). The phylogenetic trees for the NopM
312 orthologs were constructed using MEGA5. The protein sequence alignment
313 was performed using MultAlin (Multiple sequence alignment by Florence Corpet
314 (http://multalin.toulouse.inra.fr/multalin/multalin.html).
315
316 Identification of Ubiquitination Sites through Mass Spectrometry
317
318 His-LjNFR5-Myc protein obtained from the ubiquitination assay with
319 *Escherichia coli* was purified using High Affinity Ni-NTA Resin (GenScript, China,
320 L00250). The protein and the beads supplemented with a protease inhibitor
321 cocktail (Yuanye, China, S25910) at 4 °C overnight. The beads were washed
322 at least five times with washing buffer (20 mM NaH_2PO_4, pH=8.0, 300 mM NaCl,
323 50 mM imidazole). Finally, the protein was were eluted by elution buffer (20 mM
324 NaH_2PO_4, pH=8.0, 300 mM NaCl, 250 mM imidazole). The protein was then
325 analyzed by Center for Protein Research (CPR) at Huazhong Agricultural
326 University. The LjNFR5 amino acid sequence and identified and non-identified
327 lysine residues are shown in Supplementary Table S3, Fig.S6 and Fig.S7.
328
329
330

331 **Results**

332

333 NopM in a Δ*nopT* mutant positively regulates rhizobial infection of *L. japonicus*

334

335 To investigate the involvement of effectors secreted by the T3SS in the
336 regulation of rhizobial infection, we generated two T3SS knockout mutants of
337 *S. fredii* NGR234, namely *ΩttsI* and *ΩnopA*. The former lacked the
338 transcriptional regulator gene *TtsI* (*ΩttsI*), and the latter lacked a component of
339 the T3SS pilus (*ΩnopA*). Surprisingly, both mutants induced a significant
340 increase in infections of *L. japonicus* (Gifu) compared to the wild-type strain
341 (Fig. 1A, Fig. 1B and Fig. S3A). These findings suggested that T3SS in NGR234
342 negatively influences rhizobial infection.

343

344 To explore the specific contribution of individual effectors to rhizobial infection,
345 we examined mutants for six putative or *bona fide* effector genes (*ΩnopJ*,
346 *ΩnopL*, *ΩnopP*, *ΩnopZ*, *ΩnopM*, Δ*nopT*) (Kimbrel et al., 2013). Compared to
347 the parent strain NGR234, the Δ*nopT* mutant showed increased numbers of
348 infection (Fig. 1C and Fig. S3B), however, no significant differences were
349 observed for other effector mutants (Fig. 1D, 1E and Fig. S3B). This suggested
350 that the impact of effectors on symbiosis was not dependent on a single effector
351 but rather on the combined consequences of their activities, acting
352 synergistically, redundantly, or antagonistically.

353

354 To identify potential effectors that positively regulate rhizobial infection in the
355 Δ*nopT* mutant, we constructed five double mutants (Δ*nopTΩnopJ*,
356 Δ*nopTΩnopL*, Δ*nopTΩnopP*, Δ*nopTΩnopZ*, Δ*nopTΩnopM*) and inoculated
357 them onto *L. Japonicus*. The Δ*nopTΩnopJ* and Δ*nopTΩnopL* double mutants
358 induced massive infections similar to Δ*nopT* (Fig. 1F and Fig. S3C), indicating
359 that NopJ and NopL in the Δ*nopT* mutant might not affect rhizobial infection. In
360 contrast, Δ*nopTΩnopP*, Δ*nopTΩnopZ*, and Δ*nopTΩnopM* double mutants

361 showed reduced infection numbers similar to the NGR234 WT strain (Fig. 1G),
362 suggesting that NopM, NopP and NopZ might act antagonistically with NopT in
363 rhizobial infection. Despite previous reports on NopM being an E3 ligase
364 involved in symbiosis regulation (Xu et al., 2018, Xin et al., 2012), its host
365 targets have not been reported. We then focused on the identification of NopM
366 targets in plants.
367
368 NopM interacts with LjNFR1 and LjNFR5
369
370 Given that NopT negatively regulates rhizobial infection by cleaving LjNFR5
371 (Bao et al., 2024) and that NopM dimerization occurs at the plasma membrane
372 (Xu et al., 2018), we hypothesized that NopM might also associate with NFRs.
373 To test this, we first conducted a luciferase complementationg assay in
374 *Nicotiana benthamiana* expression system. A ubiquitin ligase inactive
375 $NopM^{C338A}$ was used in these experiments, because enzymatically active NopM
376 induces cell death in *N. benthamiana* cells (Xu et al., 2018). The results showed
377 that $NopM^{C338A}$ was indeed associated with both LjNFR1 and LjNFR5, as
378 indicated by strong luciferase activity when proteins were co-expressed in *N.*
379 *benthamiana* leaves (Fig. 2A and 2B). Further validation through a bimolecular
380 fluorescence complementation (BiFC) assay confirmed the interaction between
381 $NopM^{C338A}$ and LjNFR1 or LjNFR5 (Fig. 2C). A co-immunoprecipitation (co-IP)
382 assay provided additional evidence supporting the interaction between
383 $NopM^{C338A}$ and LjNFR1 or LjNFR5 (Fig. 2D, 2E). For a subsequent *in vitro* pull-
384 down assay, the cytosolic domain (CD) of LjNFR1 or LjNFR5 was co-expressed
385 with NopM in *Escherichia coli* cells and it was found that NopM indeed
386 physically interacted with Both $LjNFR1^{CD}$ and $LjNFR5^{CD}$ (Fig. 2F, 2G).
387
388 NopM ubiquitinates LjNFR5
389
390 Since NopM is an E3 ligase (Xin et al., 2012), we wondered whether NopM can

391 ubiquitinate NFRs. To test this, a ubiquitination assay was carried out using a
392 reconstituted ubiquitination cascade system (E1, E2, E3 enzymes and ubiquitin)
393 expressed in *E. coli* cells (Han et al., 2017). As shown in Fig. 3A, NopM, but not
394 $NopM^{C338A}$, exhibited autoubiquitination activity, which is consistent with
395 previous studies (Xu et al., 2018). Next, NopM was co-expressed with LjNFR5
396 in *E. coli* cells.The result showed that NopM could ubiquitinate $LjNFR5^{CD}$ as
397 strong smear protein bands were visible on immunoblots. The strong smear
398 bands of $LjNFR5^{CD}$ suggested that $LjNFR5^{CD}$ might be poly-ubiquitinated (Fig.
399 3A). Interestingly, NopM did not ubiquitinate $LjNFR1^{CD}$ (Fig. 3B). These findings
400 indicated that NopM selectively ubiquitinates LjNFR5.
401
402 Next, we wondered whether the ubiquitination of LjNFR5 by NopM is a
403 conserved mechanism that also occurs in other symbiotic interactions. We first
404 phylogenetically analyzed NopM sequences from different rhizobium species.
405 Amino acid sequence comparisons showed that the NopM proteins can be
406 divided into three clades (Fig. S4). NopMs of *Bradyrhizobium diazoefficiens*
407 USDA110 and *S. fredii* HH103 were located in Clade I and Clade III,
408 respectively. NopM of *S. fredii* NGR234 was located in Clade II. Two *NopM*
409 genes, named $NopM1_{USDA110}$ and $NopM2_{USDA110}$ were present in the USDA110.
410 *S. fredii* HH103 possesses two NopM genes with identical sequences. A
411 multiple sequence alignment indicated that C-terminal E3 ligase domain of
412 NopM was conserved whereas the length of the N-terminal Leucine-Rich
413 Repeats domain was different among three NopM clades (Fig. S5). We then
414 examined the ubiquitination of soybean $GmNFR5^{CD}$ by $NopM1_{USDA110}$ and
415 $NopM2_{USDA110}$ (Clade I) and $NopM_{HH103}$ (clade III). The results showed that
416 these three NopMs could ubiquitinate $GmNFR5^{CD}$ (Fig. 3C). These findings
417 suggested that NopM homologs from different rhizobium species exhibited a
418 conserved activity in ubiquitinating NFR5 proteins.
419
420 Expression of NopM in *L. japonicus* increases LjNFR5 protein levels

421

422 Ubiquitination is an important post-translational modification that controls
423 protein levels by mediating protein degradation or stability (Smalle and Vierstra,
424 2004). To assess whether NopM-mediated ubiquitination regulates LjNFR5
425 protein levels *in vivo*, we expressed *NopM* and *NopM*^{C338A} under the control of
426 a *Ubiquitin* promoter in hairy roots of stable transgenic *L. japonicus* expressing
427 LjNFR5-HA. LjNFR5 was detected at higher levels in NopM-expressing roots
428 than those in roots expressing NopM^{C338A} (Fig. 4A and 4B). These findings
429 indicated that the ubiquitination of LjNFR5 by NopM did not cause degradation,
430 but rather led to increased LjNFR5 protein levels.

431

432 Given that ubiquitination of LjNFR5 lead to its stability, we proposed that NopM-
433 mediated ubiquitination might form mono-ubiquitination chains. To investigate
434 the type of ubiquitin-chain linkage on LjNFR5, we utilized the Ub^{K0} variant (all
435 lysine residues in ubiqutin were substituted to arginine) (Ma et al., 2020).
436 Interestingly, the ubiquitination pattern of LjNFR5 in presence of Ub^{K0} remained
437 similar to that with ubiquitin, suggesting that LjNFR5 might be mono-
438 ubiquitinated by NopM (Fig. 4C). Accordingly, mass spectrometry analysis of
439 LjNFR5 identified ten potential ubiquitinated lysine residues (Fig. S6 and Fig.
440 S7). LjNFR5^{10KR}, a mutant version of LjNFR5 with ten lysine residues
441 substituted to arginine residues, still interacts with NopM (Fig. S8A and S8B)
442 and did not abolish the ubiquitination by NopM (Fig. 4D). However, when using
443 the Ub^{K0} variant, LjNFR5 ubiquitination was dramatically reduced (Fig. 4D),
444 suggesting that LjNFR5 still contains additional lysine residues that can be
445 either mono- or poly-ubiquitinated.

446

447 To assess the impact of ubiquitinated lysine residues on LjNFR5 function, a cell
448 death test was performed within *N. benthamiana* leaves that depends on co-
449 expression of NFRs. Co-expression of LjNFR1 with LjNFR5 iinduces a rapid
450 cell death as reported previously (Madsen et al., 2011). Co-expression of

451 LjNFR1 with LjNFR5^{10KR} caused a similar cell death response (Fig. S8C). We
452 then generated transgenic hairy roots of *L. japonicus* (Gifu) *nfr5* mutant plants
453 that expressed *LjNFR5* or *LjNFR5^{10KR}* driven by the native promoter
454 (*proLjNFR5:LjNFR5*, *proLjNFR5:LjNFR5^{10KR}*). When inoculated with GFP-
455 labelled NGR234, hairy roots transformed with the *proLjNFR5: LjNFR5^{10KR}*
456 construct showed barely infection events whereas numerous infections were
457 observed in roots expressing the LjNFR5 (Fig. S8D). These findings indicate
458 that specific lysine residues required for ubiquitinatio in LjNFR5 are essential
459 for LjNFR5 to activate symbiotic signaling.
460
461 NopM promotes rhizobial infection and nodule primordia formation
462
463 To examine the role of NopM in symbiotic response, we transformed *L.*
464 *japonicus* MG20 plants with *NopM* driven by *CaMV 35S* or *Ubiquitin* promoters.
465 Unfortunately, we could not obtain stable transgenic plants with these
466 constructs, suggesting that constitutive NopM expression might have a
467 negative effect on plant growth. We therefore generated *L. japonicus* MG20
468 plants expressing *NopM* driven by *LjNIN* promoter (*proNIN:NopM*), whose
469 activity is induced during symbiosis (Fig. S9 A-C). Two independent lines were
470 obtained and inoculated with a GFP-tagged *Mesorhizobium loti* MAFF303099
471 which does not contain *NopT* and *NopM* genes in its genome. As shown in Fig.
472 5A, 5D and Fig. S9D, increased infection foci and infection threads were
473 observed in these transgenic plants compared to control plants. Consistent with
474 this, transgenic plants also formed more nodule primordia than with wild type
475 plants at 14 dpi (Fig. 5B). Finally, to corroborate these results, we generated
476 transgenic roots expressing *NopM* driven by *Ubiquitin* promoter. Upon
477 inoculation with GFP-tagged *M. loti*, the number of rhizobial infections in these
478 *NopM*-expressing roots was significantly higher than in control roots
479 transformed with the control vector (Fig. 5C). Taken together, these data
480 indicate that NopM positively regulates rhizobial infection and nodule primordia

formation in *L. japonicus*.

Discussion

The study of type III secretion system (T3SS) effectors in gram-negative bacteria has primarily focused on their role in promoting pathogenic infections in plants. While there are parallels between the processes of rhizobial infection and colonization and those of pathogenic bacteria, the specific functions of rhizobial effectors in manipulating the plant symbiotic pathway have remained elusive. This overall aim of study was to unravel the mechanisms by which T3SS effectors regulate rhizobium-legume symbiosis. This research demonstrated that the rhizobial effector NopM can associate with two key receptors, LjNFR1 and LjNFR5, essential for activating symbiotic signaling in plants. NopM selectively ubiquitinates LjNFR5, leading to increased protein levels and enhanced rhizobial infection. These findings suggested a regulatory model in which NopM targets NFR5 in legumes to promote the symbiotic signaling transduction by altering the stability of NFR5.

Root infection by rhizobia often depends on a mixture of T3SS effectors which may act redundantly, synergistically, or antagonistically within host cells. Accordingly, mutations of effector genes show positive, negative or no effects on symbiosis with a given host plant. Analysis of rhizobial double mutants may reveal the symbiotic role of an effector that would not have been visible by mutating a single effector gene. While mutation of *nopT* in NGR234 had a positive effect on infections of *L. japonicus* roots, mutation of other effector genes did not result in an altered phenotype. However, mutation of *nopM, nopP and nopZ* in the *nopT* mutant resulted in reduced infection numbers, indicating that the symbiosis promoting effect of these effector genes was only observed in double mutants. This suggests that NopT and NopM work antagonistically, with a possiblity sharing the same target protein from hosts, to precisely

511 regulate rhizobial infection. The observed asymbiotic role of NopT may be due
512 to interactions with NFRs (Bao et al., 2024) or protein kinases related to
513 effector-triggered immunity (Khan et al., 2022, Li et al., 2023). Similar to NopT,
514 we report here that NopM can interact with the LjNFR1 and LjNFR5 of *L.*
515 *japonicus.* The findings suggest that NopT and NopM play antagonistically
516 redundant roles to fine-tune rhizobial infection in host plants.
517
518 LjNFR1 and LjNFR5 play vital roles in perceiving rhizobial NFs, activating
519 symbioti signaling in *L. japonicus* (Radutoiu et al., 2003, Madsen et al., 2011).
520 Once NF signaling is initiated, protein turnover and signaling activity of NFRs
521 may be critical for maintaining proper symbiotic signaling and subsequent
522 rhizobial infection. Previous research demonstrated that mutation in the
523 *LjPUB13* gene suppresses nodulation in *L. japonicus* (Tsikou et al., 2018).
524 LjPUB13 is an E3 ligase that interacts with and ubiquitinates LjNFR5 *in vitro*
525 (Tsikou et al., 2018). Thus, the biological role of LiPUB13 in promoting rhizobial
526 symbiosis may be similar to that of NopM, as both proteins can ubiquitinate
527 LjNFR5. In general, proteins with K48-linked polyubiquitin chains are rapidly
528 degraded, whereas proteins with other polyubiquitin chains and mono-
529 ubiquitinated proteins are not degraded and often exhibit altered properties
530 (Zhou & Zeng, 2017). In our study, we demonstrate that NopM can mono-
531 ubiquitinate LjNFR5 to stabilize LjNFR5, promoting rhizobial infection in *L.*
532 *japonicu*s. Hairy roots of *LjNFR5-HA* transgenic plants expressing
533 *proUbiquitin:NopM* showed increased LjNFR5 protein levels when compared to
534 those transformed with *proUbiquitin:NopM*^{C338A}). Although poly-ubiquitination of
535 LjNFR5 by NopM was detected at weak levels, the mono-ubiquitination of
536 LjNFR5 might be major reason leading to increased protein levels. It is therefore
537 tempting to speculate that NopM preferentially monoubiquitinates LjNFR5
538 and/or that ubiquitinated LjNFR5 contains polyubiquitin chains without K48-
539 linkages.
540

541 Pathogens utilize effectors to facilitate infection by suppressing host immunity,
542 exemplified by the E3 ubiquitin ligase effector AvrPtoB in *Pseudomonas*
543 *syringae*. AvrPtoB regulates flagellin receptor FLS2 (Goehre et al., 2008) and
544 chitin receptor CERK1 (Gimenez-Ibanez et al., 2009) protein stability in
545 *Arabidopsis thaliana*, leading to suppression of PTI. Similarly, NopM may
546 employ a similar strategy to support infection during symbiosis to avoid PTI.
547 NopM dampens the flg22-induced ROS burst in *N. benthamiana* (Xin et al.,
548 2012) and induces cell death in tobacco *via* its E3 ligase activity (Xu et al., 2018).
549
550 On the other hand, NopM activity in certain plant cells appears to induce
551 responses that are related to ETI: (i) The difficulties we observed in the
552 production of MG20 plants constitutively expressing NopM indicate negative
553 effects of NopM on plant development under certain physiological conditions.
554 (ii) NopM of NGR234 expressed in tobacco induces rapid cell death, which
555 depends on the E3 ubiquitin ligase activity (Xu et al., 2018). (iii) Mutant analysis
556 showed that NopM of *Bradyrhizobium elkanii* USDA61 triggers ETI-like early
557 nodule senescence in MG20 (Kusakabe et al., 2020). (iv) Hairy roots of MG20
558 transformed with a construct containing *NopM* of NGR234 and a tandem *CaMV*
559 *35S* promoter formed fewer nodules than plants expressing cnotrol vectors or
560 a $NopM^{C338A}$ construct (Xu et al., 2018). Thus, although NopM promotes
561 rhizobial infection and nodule primordia formation shown in this study, the
562 ubiquitin ligase activity of NopM appears to have negative effects on nodulation
563 at later stages of the symbiosis. Host plants may use ETI as a mechanism to
564 avoid unfavorable rhizobia strains.
565
566 Furthermore, another hypothetical aspect is worth mentioning. In NGR234
567 cultures treated with host flavonoids, genes related to the TTSS are later
568 expressed than *nod* genes required for Nod factor synthesis (Perret et al., 1999).
569 Thus, it can be assumed that effectors are translocated into host cells in which
570 symbiotic signaling might have already started. Because Nod factor receptors

can be viewed as gatekeepers controlling symbiotic signaling transduction, the precise regulation on Nod factor receptors could be the most effective mean by rhizobium to fine-tune symbiotic signaling in host cells. NopT of NGR234 has been found to proteolyze LjNFR5 and to inhibit symbiotic infection (Bao et al., 2024), while in our study NopM positively affected LjNFR5 levels and promoted infection by rhizobia. Mutual regulation on NFR5 by two effectors from the same rhizobium might lead to an optimized or suboptimal infection depending on the host plant.

Acknowledgments

We thank Jens Stougaard (Aarhus University) for providing *nfr5* mutant and *proNIN:GUS* transgenic seeds. We also thank Dongping Lv (Shanghai Jiaotong University) for providing bacterial ubiquitination system strains. This work was supported by the National Key R&D Program of China (2019YFA0904700), the National Natural Science Foundation of China (32090063). The qPCR and microscopy data were acquired from the Core Facility Center run by the National Key Lab of Agricultural Microbiology. Mass spectrometry analysis was performed by the Center for Protein Research at Huazhong Agricultural University.

Competing Interests

None declared.

Author Contributions: Y.W., D.X., C.S., and Y.C. conceived the idea and designed the research, Y.W., H.B., Y.L., and L.Y. performed experiments; Y.W., H.B., H.Z., and Y.C. analyzed the data, H. L. performed the bioinformatic analysis; C.S. provided some rhizobium mutants; Y.W. and Y.C wrote the manuscript; C.S. provided precious ideas and revised the manuscript.

601

602 **Data availability**

603

604 All data in this study are included in the main text or in the Supporting
605 Information.

606

607 **References**

608

609 **Büttner, D., Nennstiel, D., Klüsener, B., and Bonas, U. 2002.** Functional
610 analysis of HrpF, a putative type III translocon protein from *Xanthomonas*
611 *campestris* pv. *vesicatoria*. *J Bacteriol* **184**: 2389-2398.

612

613 **Bartsev, A.V., Deakin, W.J., Boukli, N.M., McAlvin, C.B., Stacey, G., Malnoe,**
614 **P., Broughton, W.J., and Staehelin, C. 2004.** NopL, an effector protein of sp
615 NGR234, thwarts activation of plant defense reactions. *Plant Physiol* **134**: 871-
616 879.

617

618 **Broughton, W.J., and Dilworth, M.J. 1971.** Control of leghaemoglobin
619 synthesis in snake beans. *Biochem J* **125**: 1075-1080.

620

621 **Dai, W.J., Zeng, Y., Xie, Z.P., and Staehelin, C. 2008.** S Symbiosis-promoting
622 and deleterious effects of NopT, a novel type 3 effector of Rhizobium sp strain
623 NGR234. *J Bacteriol* **190**: 5101-5110.

624

625 Deakin, W.J., and Broughton, W.J. 2009. Symbiotic use of pathogenic
626 strategies: rhizobial protein secretion systems. *Nat. Rev. Microbiol* **7**: 312-320.

627

628 **Deakin, W.J., Marie, C., Saad, M.M., Krishnan, H.B., and Broughton, W.J.**
629 **2005.** NopA is associated with cell surface appendages produced by the type
630 III secretion system of Rhizobium sp. strain NGR234. *Mol Plant Microbe*

631 *Interact* **18**: 499-507.
632
633 **Feng, Y., Wu, P., Liu, C., Peng, L.W., Wang, T., Wang, C., Tan, Q., Li, B.X.,**
634 **Ou, Y.J., Zhu, H., et al. 2021.** Suppression of LjBAK1-mediated immunity by
635 SymRK promotes rhizobial infection in *L. japonicus*. *Mol. Plant* **14**: 1935-1950.
636
637 **Figurski, D.H., and Helinski, D.R. 1979.** Replication of an origin-containing
638 derivative of plasmid Rk2 dependent on a plasmid function provided in trans.
639 *Proc Natl Acad Sci USA* **76**: 1648-1652.
640
641 **Ge, Y.Y., Xiang, Q.W., Wagner, C., Zhang, D., Xie, Z.P., and Staehelin, C.**
642 **2016.** The type 3 effector NopL of Sinorhizobium sp. strain NGR234 is a
643 mitogen-activated protein kinase substrate. *J Exp Bot* **67**: 2483-2494.
644
645 **Gimenez-Ibanez, S., Hann, D.R., Ntoukakls, V., Petutschnig, E., Lipka, V.,**
646 **and Rathjen, J.P. 2009.** AvrPtoB targets the LysM receptor kinase CERK1 to
647 promote bacterial virulence on plants. *Curr Biol* **19**: 423-429.
648
649 **Goehre, V., Spallek, T., Haeweker, H., Mersmann, S., Mentzel, T., Boller, T.,**
650 **de Torres, M., Mansfield, J.W., and Robatzek, S. 2008.** Plant pattern-
651 recognition receptor FLS2 is directed for degradation by the bacterial ubiquitin
652 ligase AvrPtoB. *Curr Biol* **18**: 1824-1832.
653
654 **Gross, J.D., and Caro, L.G. 1966. DNA transfer in bacterial conjugation.** *J*
655 *Mol Biol* **16**: 269-284.
656
657 **Han, Y.F., Sun, J.H., Yang, J., Tan, Z.Y., Luo, J.J., and Lu, D.P. 2017.**
658 Reconstitution of the plant ubiquitination cascade in bacteria using a synthetic
659 biology approach. *Plant J* **91**: 766-776.
660

Handberg, K., and Stougaard, J. 1992. *Lotus japonicus*, an autogamous, diploid legume species for classical and molecular-genetics. *Plant J* **2**: 487-496.

Heckmann, A.B., Sandal, N., Bek, A.S., Madsen, L.H., Jurkiewicz, A., Nielsen, M.W., Tirichine, L., and Stougaard, J. 2011. Cytokinin induction of root nodule primordia in *Lotus japonicus* is regulated by a mechanism operating in the root cortex. *Mol Plant Microbe Interact* **24**: 1385-1395.

Khan, A., Wadood, S.F., Chen, M., Wang, Y., Xie, Z.P., and Staehelin, C. 2022. Effector-triggered inhibition of nodulation: A rhizobial effector protease targets soybean kinase GmPBS1-1. *Plant Physiol* **189**: 2382-2395.

Kimbrel, J.A., Thomas, W.J., Jiang, Y., Creason, A.L., Thireault, C.A., Sachs, J.L., and Chang, J.H. 2013. Mutualistic co-evolution of type III effector genes in *Sinorhizobium fredii* and *Bradyrhizobium japonicum*. *PLoS Pathog* **9**: e1003204.

Kusakabe, S., Higasitani, N., Kaneko, T., Yasuda, M., Miwa, H., Okazaki, S., Saeki, K., Higashitani, A., and Sato, S. 2020. Accessions possess multiple checkpoints triggered by different type III secretion system effectors of the wide-host-range symbiont USDA61. *Microbes Environ* **35**: 2020.

Li, D.D., Zhu, Z.K., Deng, X.M., Zou, J.N., Ma, C., Li, C.D., Yin, T., Liu, C.Y., Wang, J.H., Chen, Q.S., et al. 2023. A hub gene interacting with rhizobial type-III effectors NopT and NopP, regulates soybean nodulation. *Agronomy-Basel* **13**: 1242.

Ma, X.Y., Claus, L.A.N., Leslie, M.E., Tao, K., Wu, Z.P., Liu, J., Yu, X., Li, B., Zhou, J.G., Savatin, D.V., et al. 2020. Ligand-induced monoubiquitination of BIK1 regulates plant immunity. *Nature* **581**: 199-203.

691

692 **Madsen, E.B., Antolín-Llovera, M., Grossmann, C., Ye, J.Y., Vieweg, S.,**
693 **Broghammer, A., Krusell, L., Radutoiu, S., Jensen, O.N., Stougaard, J., et**
694 **al. 2011.** Autophosphorylation is essential for the function of the Nod factor
695 receptor 1 and receptor-mediated signaling in cooperation with Nod factor
696 receptor 5. *Plant J* **65**: 404-417.

697

698 **Marie, C., Deakin, W.J., Viprey, V., Kopciñska, J., Golinowski, W., Krishnan,**
699 **H.B., Perret, X., and Broughton, W.J. 2003.** Characterization of Nops,
700 nodulation outer proteins, secreted via the type III secretion system of NGR234.
701 *Mol. Plant Microbe Interact* **16**: 743-751.

702

703 **Perret, X., Freiberg, C., Rosenthal, A., Broughton, W.J., and Fellay, R. 1999.**
704 High-resolution transcriptional analysis of the symbiotic plasmid of Rhizobium
705 sp. NGR234. *Mol Microbiol* **32**: 415-425.

706

707 **Quandt, J., and Hynes, M.F. 1993.** Versatile suicide vectors which allow direct
708 selection for gene replacement in gram-negative bacteria. *Gene* **127**: 15-21.

709

710 **Radutoiu, S., Madsen, L.H., Madsen, E.B., Felle, H.H., Umehara, Y.,**
711 **Gronlund, M., Sato, S., Nakamura, Y., Tabata, S., Sandal, N., et al. 2003.**
712 Plant recognition of symbiotic bacteria requires two LysM receptor-like kinases.
713 *Nature* **425**: 585-592.

714

715 **Saad, M.M., Kobayashi, H., Marie, C., Brown, I.R., Mansfield, J.W.,**
716 **Broughton, W.J., and Deakin, W.J. 2005.** NopB, a type III secreted protein of
717 Rhizobium sp. strain NGR234, is associated with pilus-like surface appendages.
718 *J Bacteriol* **187**: 1173-1181.

719

720 **Skorpil, P., Saad, M.M., Boukli, N.M., Kobayashi, H., Ares-Orpel, F.,**

721 **Broughton, W.J., and Deakin, W.J. 2005.** NopP, a phosphorylated effector of
722 Rhizobium sp. strain NGR234, is a major determinant of nodulation of the
723 tropical legumes *Flemingia congesta* and *Tephrosia vogelii*. *Mol Microbiol* **57**:
724 1304-1317.
725
726 **Smalle, J., and Vierstra, R.D. 2004.** The ubiquitin 26S proteasome proteolytic
727 pathway. *Annu Rev Plant Biol* **55**: 555-590.
728
729 **Teulet, A., Camuel, A., Perret, X., and Giraud, E. 2022.** The versatile roles of
730 type III secretion systems in rhizobium-legume symbioses. *Annu Rev Microbiol*
731 **76**: 45-65.
732
733 **Tsikou, D., Ramirez, E.E., Psarrakou, I.S., Wong, J.E., Jensen, D.B., Isono,**
734 **E., Radutoiu, S., and Papadopoulou, K.K. 2018.** A E3 ligase interacts with
735 the Nod Factor Receptor 5 and positively regulates nodulation. *BMC Plant Biol*
736 **18**: 217.
737
738 **Waadt, R., Schmidt, L.K., Lohse, M., Hashimoto, K., Bock, R., and Kudla,**
739 **J. 2008.** Multicolor bimolecular fluorescence complementation reveals
740 simultaneous formation of alternative CBL/CIPK complexes. *Plant J* **56**: 505-
741 516.
742
743 **Wang, L., Yu, G., Macho, A.P., and Lozano-Duran, R. 2021.** Split-luciferase
744 complementation imaging assay to study protein-protein interactions in
745 *Nicotiana benthamiana*. *Bio Protoc* **11**: e4237.
746
747 **Wassem, R., Kobayashi, H., Kambara, K., Le Quere, A., Walker, G.C.,**
748 **Broughton, W.J., and Deakin, W.J. 2008.** TtsI regulates symbiotic genes in
749 Rhizobium species NGR234 by binding to tts boxes. *Mol Microbiol* **68**: 736-748.
750

751 **Xin, D.W., Liao, S., Xie, Z.P., Hann, D.R., Steinle, L., Boller, T., and Staehelin,**
752 **C. 2012.** Functional analysis of NopM, a novel E3 ubiquitin ligase (NEL) domain
753 effector of Rhizobium sp. strain NGR234. *PLoS Pathog* **8**: e1002707.
754
755 **Xu, C.C., Zhang, D., Hann, D.R., Xie, Z.P., and Staehelin, C. 2018.**
756 Biochemical properties and in planta effects of NopM, a rhizobial E3 ubiquitin
757 ligase. *J Biol Chem* **293**: 15304-15315.
758
759 **Yang, J., Lan, L., Jin, Y., Yu, N., Wang, D., and Wang, E. 2022.** Mechanisms
760 underlying legume-rhizobium symbioses. *J Integr Plant Biol* **64**: 244-267.
761
762 **Zhou, B.J., and Zeng, L.R. 2017.** Conventional and unconventional
763 ubiquitination in plant immunity. *Mol Plant Pathol* **18**: 1313-1330.
764
765 **Supporting Information**
766
767 Fig. S1. Schematic of NGR234 Mutants.
768
769 Fig. S2. PCR Analysis of NGR234 Mutants.
770
771 Fig. S3. GUS Staining Pictures for Roots of *L. japonicus* Inoculated with *S. fredii*
772 NGR234 and Mutant Strains.
773
774 Fig. S4. Phylogenetic Tree of NopM Homologs in Different Rhizobial Species.
775
776 Fig. S5. Amino Acid Sequence Alignment of NopM Homologous in Different
777 Rhizobial Species.
778
779 Fig. S6. Amino Acid Sequence of LjNFR5 with Identified Lysine Ubiquitination
780 Sites.

Fig. S7. *In Vitro* Ubiquitination Sites of LjNFR5 Identified by Mass Spectrometry.

Fig. S8. LjNFR5^{10KR} Does Not Affect Interactions with Nod Factor Receptors but Is Symbiotically Inactive.

Fig. S9. Detection of *NopM* DNA, *NopM* Expression and NopM Protein in Transgenic Plants

Table S1. Primers Used in This Study.

Table S2. Mutants of *S. fredii* NGR234 Constructed in This Study.

Table S3. LjNFR5 *In Vitro* Ubiquitination Sites Identified by Mass Spectrometry.

Figures

Figure 1. Infection Numbers of *L. japonicus* Roots Inoculated with NGR234 and Mutant Strains.

The number of rhizobial infections formed on *L. japonicus* (Gifu) roots inoculated with *S. fredii* NGR234 wild-type and mutants at 6 dpi, (A) NGR234 (n=8) and *ΩttsI* (n=8); (B) NGR234 (n=8) and *ΩnopA* (n=8); (C) NGR234 (n=8) and *ΔnopT* (n=8); (D) NGR234 (n=10) and *ΩnopM* (n=10); (E) NGR234 (n=8), *ΩnopJ* (n=7), *ΩnopL* (n=7), *ΩnopP* (n=8), and *ΩnopZ* (n=8); (F) NGR234 (n=8), *ΔnopT* (n=5), *ΔnopTΩnopJ* (n=5), and *ΔnopTΩnopL* (n=5); (G) NGR234 (n=5), *ΔnopT* (n=5), *ΔnopTΩnopM* (n=5), *ΔnopTΩnopP* (n=5), and *ΔnopTΩnopZ* (n=5). All the rhizobia were labeled with GFP markers. Data are mean ± SD (Student's t-test, P < 0.01; ns, not significant).

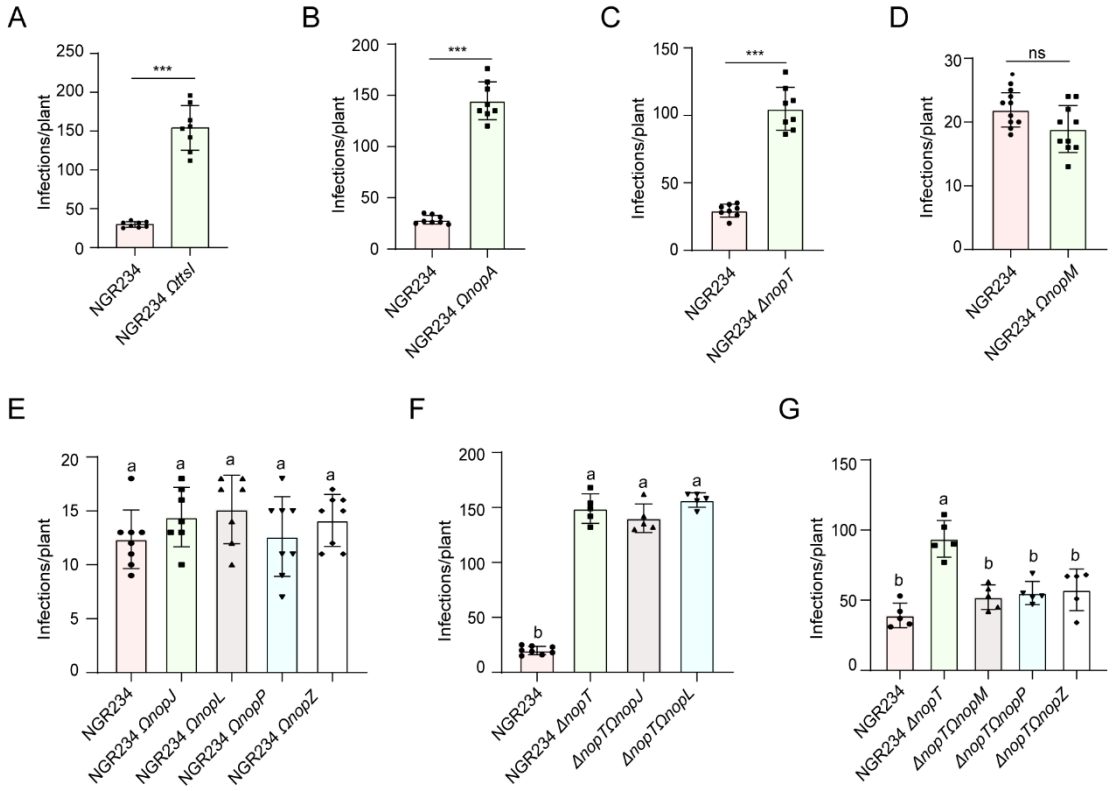

Figure 2. NopM Interacts with LjNFR1 and LjNFR5.

(A) and (B) NopM interacts with LjNFR5 or LjNFR1 in split-luciferase assay. NopM^{C338A}-nLUC was co-expressed with LjNFR5-cLUC and LjNFR1-cLUC in *N. benthamiana* leaves. NopM^{C338A}-nLUC and AtFLS2-cLUC are negative controls, whileLjNFR5-cLUC and LjNFR1^{K351E}-nLUC (kinase-dead) served as a positive control. The combination NopM^{C338A}-nLUC with NopM^{C338A}-cLUC was also analyzed.Luminescence signals indicate protein–protein interactions.

(C) NopM interacts with LjNFR5 or LjNFR1 in BiFC assay. NopM^{C338A}-nYFP was co-expressed with LjNFR5-cYFP or LjNFR1-cYFP in *N. benthamiana*, and fluorescence was visualized by confocal microscopy. Negative controls included NopM^{C338A}-nYFP with AtFLS2-cYFP. The combination NopM^{C338A}-nYFP with NopM^{C338A}-cYFP was also examined. Bar=25 μm.

(D) and (E) NopM interacts with LjNFR5 or LjNFR1 inCo-immunoprecipitation (co-IP) assay. LjNFR5-GFP and LjNFR1-GFP were immunoprecipitated with anti-GFP antibody and detected by immunoblotting with anti-FLAG antibody.

(F) and (G) NopM physically interacts LjNFR5 or LjNFR1 in pull-down assay. MBP-LjNFR5-Myc, MBP-LjNFR1-Myc, and NopM were co-expressed in *E. coli* cells. Pull-down was performed with amylose resin and detected by immunoblotting with anti-NopM and anti-Myc antibodies.

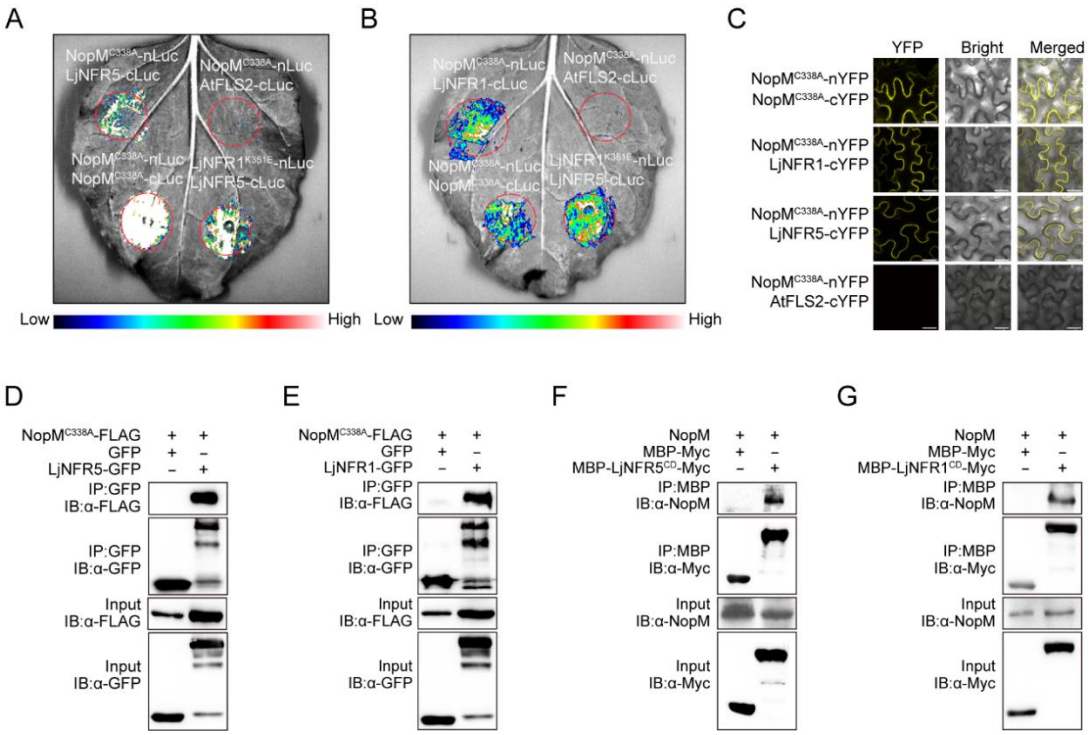
A
NopM^{C338A}-nLuc
LjNFR5-cLuc
NopM^{C338A}-nLuc
AtFLS2-cLuc
NopM^{C338A}-nLuc
NopM^{C338A}-cLuc
LjNFR1^{K351E}-nLuc
LjNFR5-cLuc
Low
High
B
NopM^{C338A}-nLuc
LjNFR1-cLuc
NopM^{C338A}-nLuc
AtFLS2-cLuc
NopM^{C338A}-nLuc
NopM^{C338A}-cLuc
LjNFR1^{K351E}-nLuc
LjNFR5-cLuc
Low
High
C
YFP
Bright
Merged
NopM^{C338A}-nYFP
NopM^{C338A}-cYFP
NopM^{C338A}-nYFP
LjNFR1-cYFP
NopM^{C338A}-nYFP
LjNFR5-cYFP
NopM^{C338A}-nYFP
AtFLS2-cYFP
D
NopM^{C338A}-FLAG + +
GFP + –
LjNFR5-GFP – +
IP:GFP
IB:α-FLAG
IP:GFP
IB:α-GFP
Input
IB:α-FLAG
Input
IB:α-GFP
E
NopM^{C338A}-FLAG + +
GFP + –
LjNFR1-GFP – +
IP:GFP
IB:α-FLAG
IP:GFP
IB:α-GFP
Input
IB:α-FLAG
Input
IB:α-GFP
F
NopM + +
MBP-Myc + –
MBP-LjNFR5^{CD}-Myc – +
IP:MBP
IB:α-NopM
IP:MBP
IB:α-Myc
Input
IB:α-NopM
Input
IB:α-Myc
G
NopM + +
MBP-Myc + –
MBP-LjNFR1^{CD}-Myc – +
IP:MBP
IB:α-NopM
IP:MBP
IB:α-Myc
Input
IB:α-NopM
Input
IB:α-Myc

835

Figure 3. NopM Ubiquitinates LjNFR5.

(A) NopM , but not NopM^{C338A}, ubiquitinates LjNFR5 in *E. coli*.. NopM or NopM^{C338A}, AtUBA1 (E1), AtUBC8 (E2), His-FLAG-Ub, and Myc tagged cytosolic domain (CD) of LjNFR5 (LjNFR5^{CD}-Myc) were co-expressed in *E. coli*. Bacterial lysates were subjected to immunoblotting using anti-FLAG, anti-Myc, and anti-NopM antibodies. Asterisks indicated non- specific band.

(B) NopM ubiquitinates LjNFR5, but not LjNFR1. LjNFR5^{CD}-Myc or LjNFR1^{CD}-Myc were co-expressed with NopM, AtUBA1 (E1), AtUBC8 (E2) and His-FLAG- Ub. Western blotting was performed with bacterial lysates using anti-Myc and anti-FLAG antibodies.

(C) Different NopM proteins from different rhizobium species ubiquitinate LjNFR5 or GmNFR5. The Myc-tagged cytosolic domain of both NFR5 (NFR5^{CD}-Myc), NopM from indicated strains, AtUBA1 (E1), AtUBC8 (E2), and His and FLAG-tagged ubiquitin (His-FLAG- Ub) were co-expressed in *E. coli*. The bacterial lysates were subjected to Western blotting using anti-FLAG and anti-Myc antibodies.

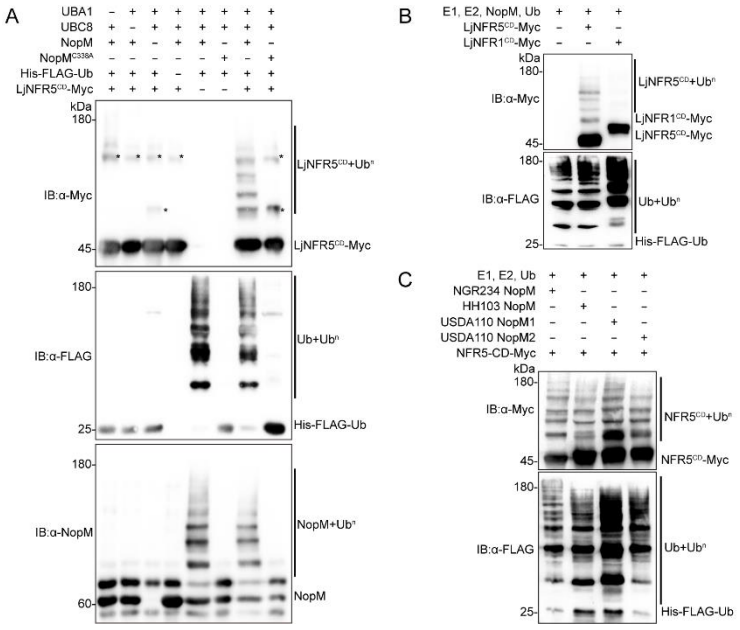

857 **Figure 4. NopM Expression in *L. japonicus* Roots Increases LjNFR5**
858 **Levels and NopM-mediated Multi-monoubiquitination of LjNFR5 with**
859 **Ub^{K0}.**
860
861 (A) NopM expression in *L. japonicus* results in increased LjNFR5 protein
862 levels. NopM-FLAG driven by the *Ubiquitin* promoter, was expressed in hairy
863 roots of *proUbiquitin:LjNFR5-HA* plants. Protein levels detected by
864 immunoblotting with anti-HA, anti-NopM, and anti-actin antibodies.(B)
865 Quantification of signals of Western blot bands shown in panel (A). Protein
866 expression levels of LjNFR5 are shown as fold change relative to actin. **$p <$
867 0.05 (Student's t-test).
868
869 (C) NopM-mediated multi-monoubiquitination of LjNFR5 with Ub^{K0} The
870 ubiquitination assay with *E. coli* cells was performed using His-Flag-tagged
871 Ub^{K0}, a ubiquitin variant with all lysine residues substituted to arginine (His-
872 Flag- Ub^{K0}) Ubiquitinated proteins were detected by immunoblotting with anti-
873 FLAG and anti-Myc. Asterisks indicated non- specific bands.
874
875 (D) A similar ubiquitination experiment was performed with $LjNFR5^{10KR}$, in
876 which ten lysine residues are substituted to arginine
877

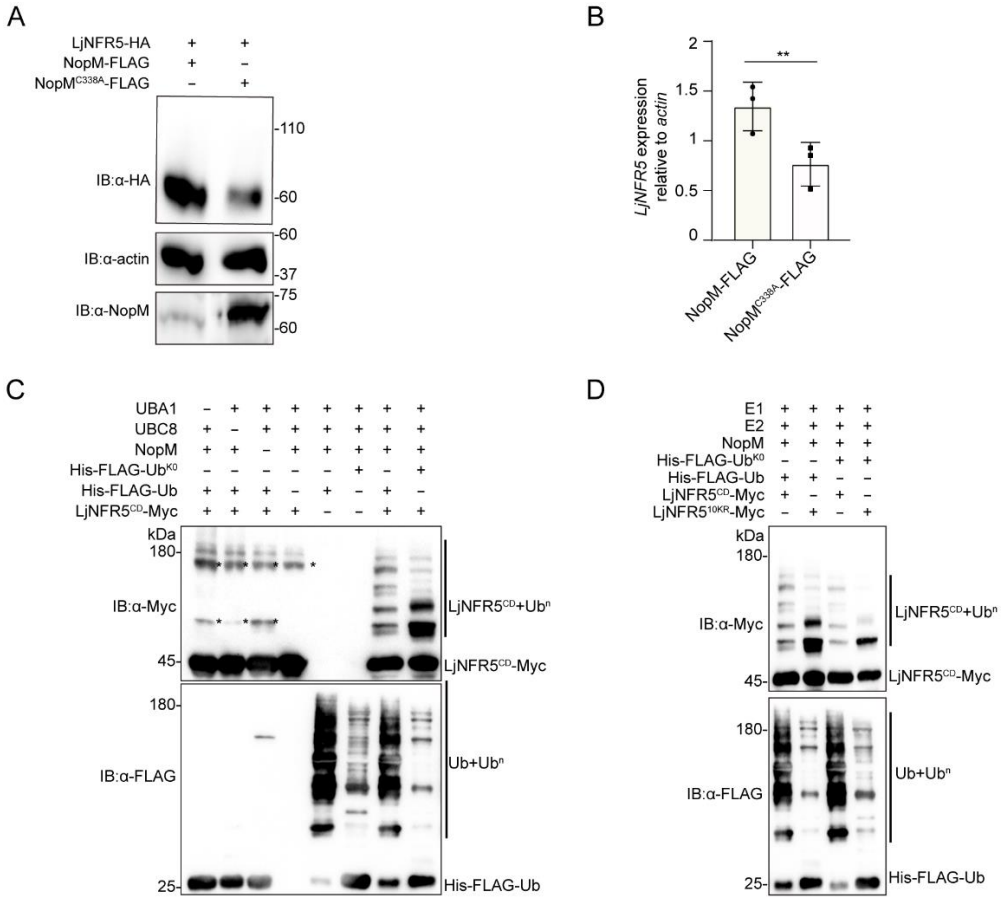
A
LjNFR5-HA + +
NopM-FLAG + –
NopM^{C338A}-FLAG – +
IB:α-HA
IB:α-actin
IB:α-NopM
110
60
60
37
75
60
B
LjNFR5 expression relative to actin
2
1.5
1
0.5
0
**
NopM-FLAG
NopM^{C338A}-FLAG
C
UBA1 – + + + + + + +
UBC8 + – + + + + + +
NopM + + – + + + + +
His-FLAG-Ub^{K0} – – – – – + – +
His-FLAG-Ub + + + – + – + –
LjNFR5^{CD}-Myc + + + + – – + +
kDa
180
IB:α-Myc
45
LjNFR5^{CD}+Ub^{n}
LjNFR5^{CD}-Myc
180
IB:α-FLAG
Ub+Ub^{n}
25
His-FLAG-Ub
D
E1 + + + +
E2 + + + +
NopM + + + +
His-FLAG-Ub^{K0} – – + +
His-FLAG-Ub + + – –
LjNFR5^{CD}-Myc + – + –
LjNFR5^{10KR}-Myc – + – +
kDa
180
IB:α-Myc
45
LjNFR5^{CD}+Ub^{n}
LjNFR5^{CD}-Myc
180
IB:α-FLAG
Ub+Ub^{n}
25
His-FLAG-Ub

878

879

880 **Figure 5. *L. japonicus* Plants Transformed with *proNIN:NopM* and**
881 **Inoculated with *M. loti* Show Increased Infection and Nodule Primordia**
882 **Formation.**
883
884 (A) The number of rhizobial infections per plant was significantly greater in
885 transgenic *L. japonicus* MG20 lines carrying the *proNIN:NopM* construct than
886 in the MG20 control plants. Roots were inoculated with GFP-labelled *M. loti*
887 303099 and microscopically analyzed at 5 dpi. Error bars represent ±SD. ***p
888 < 0.01 (Student's t-test, n=8).
889
890 (B) Nodule primordia number per plant were counted in *proNIN:NopM* lines
891 inoculated with GFP-labelled *M. loti* when analyzed at 14 dpi with *M. loti*.
892 Data are mean ±SD (***p < 0.01, Student's t-test; MG20, n=12; *proNIN:*
893 *NopM*-1, n=11; *proNIN: NopM*-2, n=9).
894
895 (C) The number of rhizobial infections per plant increased significantly in hairy
896 roots of *L. japonicus* MG20 carrying the *proUbiquitin:NopM* construct as
897 compared to the empty vector control (EV). Roots were microscopically
898 analyzed at 5 dpi. Error bars represent ±SD. ***p < 0.01 (Student's t-test;
899 MG20, n=8; *proUbiquitin:NopM*, n=5).
900
901 (D) Microscopic images illustrating rhizobial root infection events (the upper
902 images were infection foci and the lower images were infection threads) in
903 MG20 wild type and *proNIN:NopM* lines (5 dpi). Fluorescent, GFP-
904 expressing *M. loti* bacteria are shown in the upper images and corresponding
905 brightfield images are presented below. Bar=200 μm. White asterisks indicate
906 bacteria in the upper images.
907

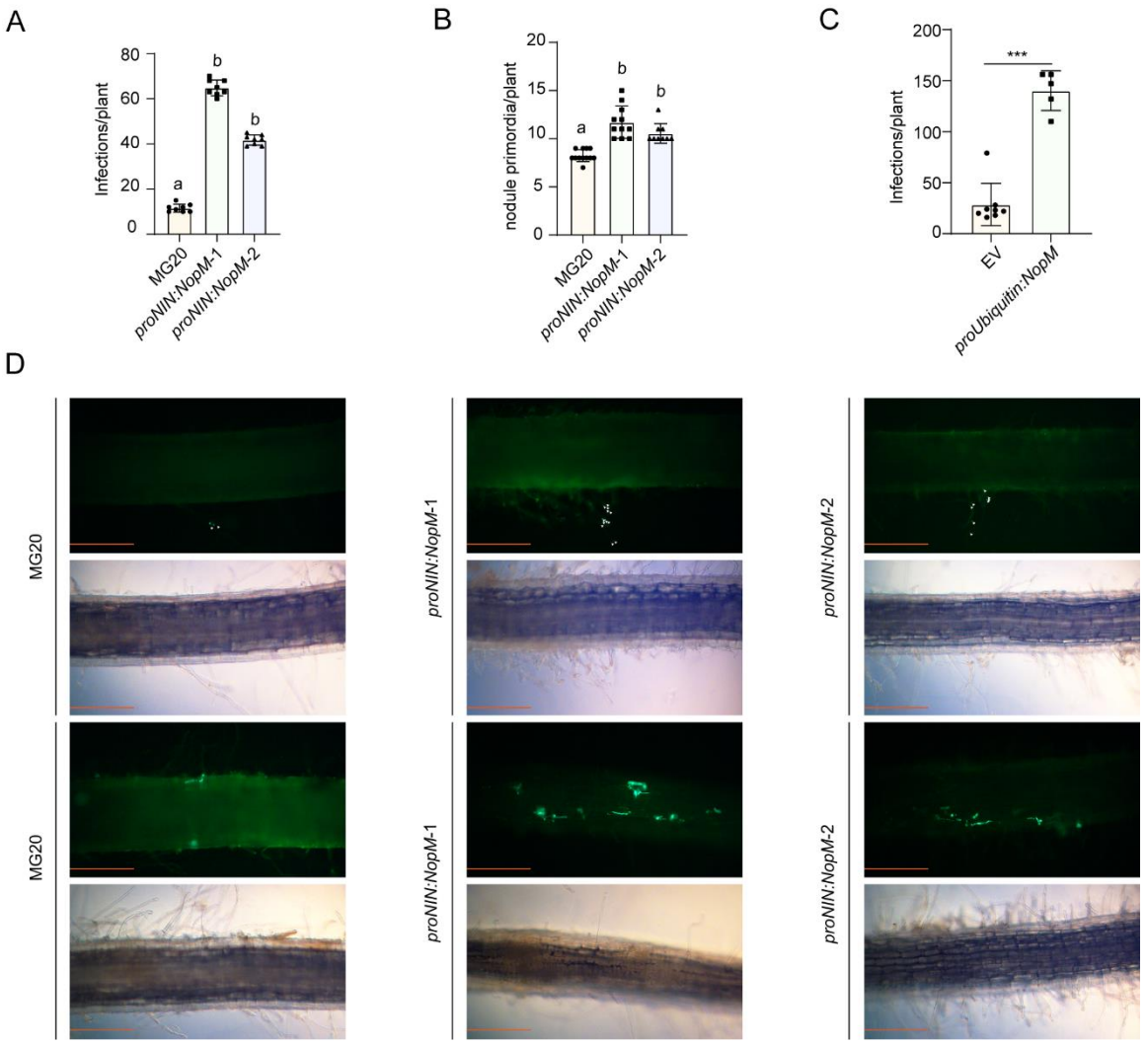
A
Infections/plant
80
60
40
20
0
a
b
b
MG20
proNIN:NopM-1
proNIN:NopM-2
B
nodule primordia/plant
20
15
10
5
0
a
b
b
MG20
proNIN:NopM-1
proNIN:NopM-2
C
Infections/plant
200
150
100
50
0
***
EV
proUbiquitin:NopM
D
MG20
MG20
proNIN:NopM-1
proNIN:NopM-1
proNIN:NopM-2
proNIN:NopM-2

908

909